# MEASUREMENT OF SOLIDS BEHAVIOUR IN A FAST FLUIDIZED BED

Toshinori KOJIMA, Ken-Ichi ISHIHARA, Yang GUILIN*
AND THE LATE Takehiko FURUSAWA

*Department of Chemical Engineering, The University of Tokyo,
Bunkyo-ku, Tokyo, 113*

The velocity and the axial dispersion of solids within a bed (50 mm in inner diameter, 3600 mm in height) with high gas velocity were analyzed by impulse response of tracer particles. FCC-particles ("group A" powder according to Geldart classification) were employed for the present investigation.

Local particle velocity at the axis of the bed increased with increased gas velocity, while the fraction of solids decreased. The axial dispersion coefficient within the bed ranged from 1 to 900 cm$^2$/s. This result suggested unsteady and random behaviour of solids within the fast fluidized bed. Local slip velocity at the axis of the bed was mostly larger than the terminal velocity of a single particle.

## Introduction

A circulating fluidized bed system is considered as an advanced alternative to conventional dense fluidized beds. The circulating fluidized bed system is composed of a "main bed" (riser) with high velocity, a fast fluidized bed, and a "companion bed" (downcomer) of a conventional fluidized bed or a moving bed. As discussed elsewhere,[15] the advantages of the circulating fluidized bed over the conventional bubbling fluidized bed are: [1] high processing capacities per unit area, [2] excellent contact between gas and solids, [3] high degree of mixing of solids, [4] plug flow condition of gas, [5] easy handling of cohesive solids and [6] easy scale-up. The system has been successfully applied to some gas-solid reaction systems including the calcination processes of aluminum hydroxide[11] and the coal combustion process,[5] where high combustion efficiency and high utilization efficiency of limestone are realized. In contrast to its increasing importance, the definition of the fast fluidization regime has not been well understood[3,13] and the behaviour of gas and solids within the bed have not been fully elucidated, while a lot of data on the volume fraction of solids, particle velocity and slip velocity have been reported.[9,14-17] Recently, the local behaviour of solids has also been measured by optical fiber probes[2,4] or sampling probe.[12]

The objective of the present paper is to investigate the behaviour of solids including axial dispersion of solids as well as volume fraction of solids and local particle velocity within a fast fluidized bed. In the present investigation, local particle velocity was directly measured by use of an optical fiber technique[6,7,10] using tracer particles with fluorescent dye.

## 1. Experimental

### 1.1 Apparatus

The circulating fluidized bed system employed in the present investigation is shown in **Fig. 1**. The vertical test section, which was usually operated under the fast fluidization condition, consisted of a 3600 mm length of acrylic transparent tubing 50 mm in inside diameter. A gas distributor plate with 220 holes 0.5 mm in diameter was installed at the bottom of the section. The particles were introduced from the companion bed to the test section at 125 mm above the distributor through acrylic tubing 50 mm in inside diameter. The tubing was inclined by 30° and equipped with a ball valve. The valve was kept full-open throughout the experiments. The taps, 25 mm in inside diameter, were located at 100, 250 and 400 mm above the distributor and at every 200 mm for the upper part above 400 mm. These taps were used for pressure measurement and tracer injection. The test section was additionally equipped with five taps of 15 mm inside diameter at every 50 mm from 1850 mm above the distributor. These taps were used for detection of tracer particles by insertion of an optical fiber probe. The entrained particles and the gas from the top of the test section were introduced to two serial cyclones
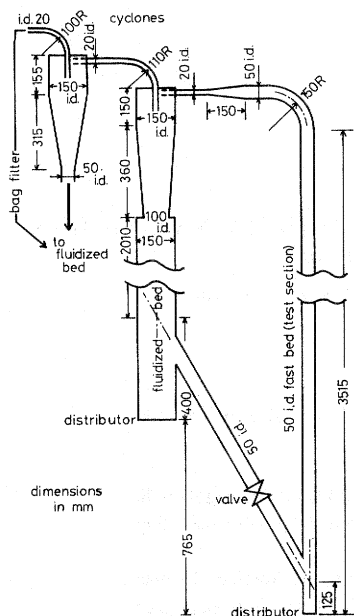
**Fig. 1.** Circulating fluidized-bed system

made of stainless steel and 150 mm in inside diameter. The gas from the cyclones was then introduced into a bag filter. Then the collected particles were returned to the companion bed, which was operated under the bubbling condition ($U_g = 3.3\ U_{mf}$). The companion bed consisted of a 2400 mm length of acrylic transparent tubing 150 mm in inside diameter and was equipped with a distributor plate having 88 holes 0.5 mm in diameter. The particles were effused from the companion bed through the inclined tubing connected at 300 mm above the distributor plate into the test section. A branched ball valve, placed in the upper part of the inclined tubing, was used to remove the particles from the system.

### 1.2 Particles

FCC particles (Shokubai Kasei Co., Ltd.) were employed for the present experimental runs. The average diameter and the particle density were respectively 0.060 mm and 1.0 g/cm$^3$, and the minimum fluidization velocity calculated was 0.12 cm/s. The total loading of the particles in the system was adjusted by particle addition into or removal from the companion bed. FCC particles treated with a fluorescent dye (Tombo Pencil Co., Ltd., peak wave length of emission spectrum: 520 nm) were used as the tracer particles.

### 1.3 Measurement of pressure gradient through test section

Longitudinal profiles of static pressure were measured by manometers for superficial gas velocities ranging from 50 to 200 cm/s. An inclined manometer was employed for measurement of the precise pressure difference between the two taps which were used for measurement of the local particle velocity by use of optical fiber probes as described in section 1.4.

Though the diameter of the test column employed for the present investigation was smaller than that employed by Yerushalmi et al.,[14] the volume fraction of solids, $1-\varepsilon$, at a certain level of the bed was evaluated from the following equation by assuming that the shear stress at the wall is negligible.[14]

$$\Delta p/\Delta z = \rho_p g(1-\varepsilon) \tag{1}$$

where $\rho_p$ is the particle density and $g$ is the acceleration of gravity. Total loading of the particles throughout the test section, excluding the particle acceleration region with a high volume fraction of solids, was also calculated from the static pressure difference between the levels 100 and 3400 mm above the distributor.

### 1.4 Measurement of local behaviour of solids under fast fluidized bed condition

The impulse of tracer particles (1.0–2.0 g) was introduced into the test section at the level 1800 mm above the distributor under the fast fluidization condition (150 cm/s $< U_g <$ 215 cm/s). The signals from the tracer particles were detected by two optical fiber probes[6,7,10] which were installed at levels 1900 and 2000 mm above the distributor of the test section. The ends of the optical fiber probes were located at the axis of the tube. Ultraviolet light was transmitted into the bed through the optical fibers and the visible light reflected from the tracer particles was in turn transmitted through the fibers and detected by photomultipliers with filters. In some experimental runs, an impulse of the tracer was also introduced at a level 1600 mm above the distributor and/or the distance between the probes was varied from 50 to 200 mm. The particle velocity calculated was hardly affected by the arrangements of the introduction point and detection points of the tracer particles. The details of the measurement system have been published elsewhere.[7]

## 2. Results and Analysis

### 2.1 General observation and axial distribution of holdup of solids

With a gas velocity increase from 50 to 100 cm/s, transition from a slugging regime to a turbulent regime was observed and the intensity of pressure fluctuation was drastically reduced. The volume fractions of solids calculated by Eq. (1) from the pressure gradient are shown in **Figs. 2** and **3** respectively for superficial gas velocities of 50 and 100 cm/s. In these two regimes a change in pressure gradient, which indicated the surface of the bed, was observed and bed height increased with increase in loading of particles in the system. The volume fraction of solids in the dense bed remained constant, however.

When the gas velocity exceeded 150 cm/s, the bed was observed to be violently agitated and descending particles were clearly observed in the vicinity of the
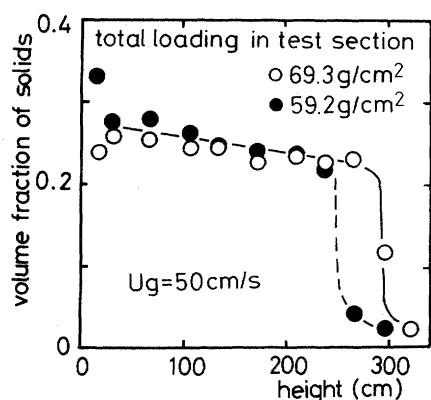
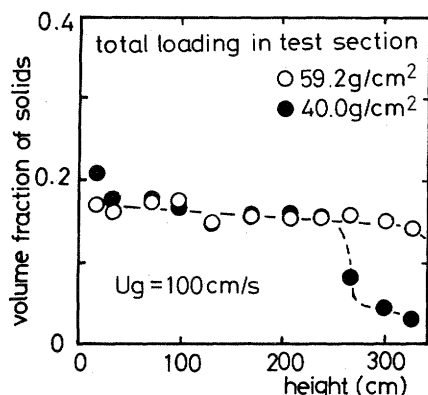**Fig. 2.** Volume fraction of solids under slugging regime ($U_g = 50$ cm/s)



**Fig. 4.** Volume fraction of solids under fast fluidization regime ($U_g = 150$ cm/s)



**Fig. 3.** Volume fraction of solids under turbulent regime ($U_g = 100$ cm/s)
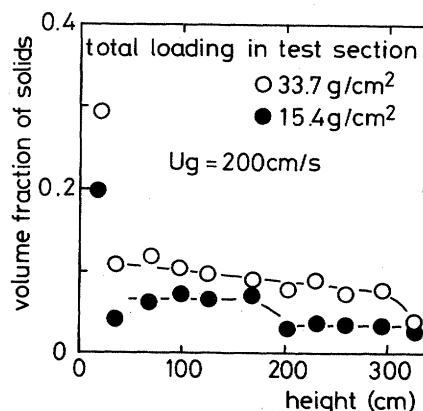


**Fig. 5.** Volume fraction of solids under fast fluidization regime ($U_g = 200$ cm/s)

wall. Visual observation suggested an intensive backmixing of solids within the bed. The volume fraction of solids was calculated by Eq. (1) and is shown in **Figs. 4** and **5** respectively for superficial gas velocities of 150 and 200 cm/s. In these figures, a sharp change in the fraction of solids or in the clear surface of the bed was no longer observed. This suggests that the bed was under the fast fluidization regime.[16] Relatively high holdup of solids was observed in the lower part of the test section (lower than a level 100–200 mm above the distributor) where the particles were accelerated. At the top of the bed where the test section was connected to the companion bed through cyclones, end effects were also observed. In the middle part of the bed (between 400 and 3000 mm above the distributor), the holdup of solids remained almost constant independently of the height above the distributor. The holdup of solids increased with increased loading of particles in the test section. Exceptionally, an obscure change in fraction of solids was observed around 2000 mm above the distributor when the total loading in the test section was lower than 25 g/cm². This may correspond to the interface or inflection point of voidage, pointed out by Youchou and Kwauk,[17] although no further discussion of the
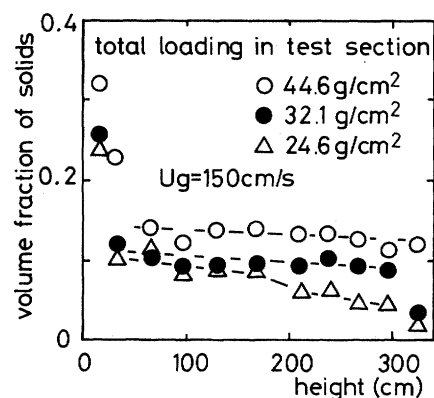
phenomenon is attempted here.

The average volume fraction of solids through the middle part of the bed (from 400 to 2000 mm above the distributor), where stable dense (lower than the bed surface) or fast fluidization was observed, is plotted against the total loading of the particles in the test section in **Fig. 6** for all of the experimental results shown in Figs. 2–5. Under the fast fluidization condition, the holdup of solids was significantly affected by the total loading in the test section, namely the total inventory of particles in the system. The holdup of solids is also affected by the circulation rate of the solids, but in the present experiments the valve was always kept full-open and the feed rate of solids from the companion bed was not controlled.

## 2.2 Analysis of signals generated by tracer particles

Typical examples of the signals generated by the tracer particles at the center of the horizontal cross section, when the tracer was introduced at a level of 1800 mm and detected at levels of 1900 and 2000 mm above the distributor, are shown in **Fig. 7**. The signals included fluctuations with a frequency of 100 Hz caused by the frequency of electric light of 50 Hz; in Fig. 7, therefore, the points of peak intensities are smoothly connected. The curve obtained was analyzed
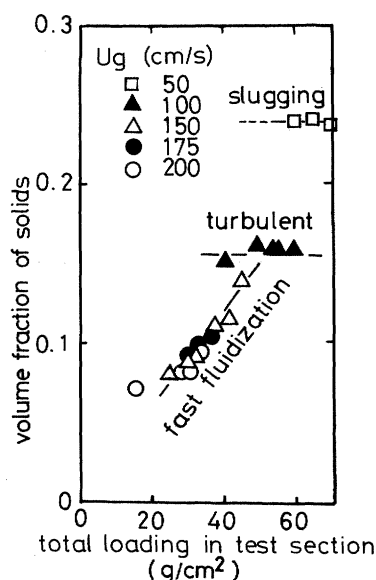
**Fig. 6.** Effect of total loading in test section on volume fraction of solids
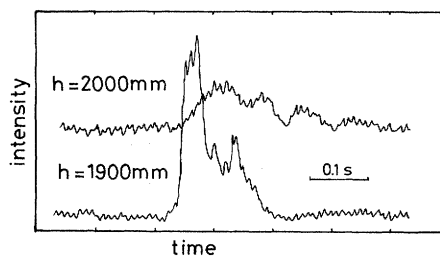


**Fig. 7.** Typical examples of reflexion signals

as follows. The intensity of the signal was assumed to be proportional to the concentration of tracer particles, i.e., to the solid concentration, $C_p$. The fluctuations of the motion of particles in the bed were analyzed by the following axial dispersion model.[1]

$$\frac{E_z}{1-\varepsilon}\frac{\partial^2 C_p}{\partial z^2}-U_p\frac{\partial C_p}{\partial z}-\frac{\partial C_p}{\partial t}=0 \qquad (2)$$

Under the open vessel condition, the particle velocity, $U_p$, is not directly given by a first absolute moment from one curve,[8] but rather by the difference between the two first moments from the two curves obtained at the different levels, $\Delta\mu_1$, as follows.

$$U_p=\Delta z/\Delta\mu_1 \qquad (3)$$

The axial dispersion coefficient, $E_z$, is also evaluated from the difference between the two second central moments from the two curves, $\Delta\mu_2$, as follows, without error for a one-shot tracer input under the present boundary condition.[8]

$$E_z=\frac{(1-\varepsilon)U_p^3\Delta\mu_2}{2\Delta z} \qquad (4)$$

where $z$ is the height and $\Delta z$ is the distance between the two detectors for the tracer particles. In the case
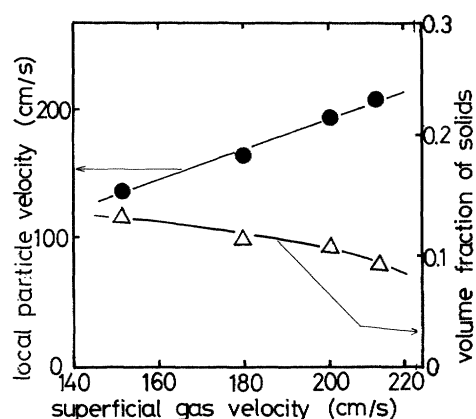


**Fig. 8.** Local particle velocity, and volume fraction of solids vs. superficial gas velocity

presented in Fig. 7, the value of $\Delta z$ was 10 cm. The first absolute moment and the second central moment at the height of $z$ are defined as follows.

$$\mu_1=\frac{\displaystyle\int_0^\infty C_p(t,z)t\,dt}{\displaystyle\int_0^\infty C_p(t,z)\,dt} \qquad (5)$$

$$\mu_2=\frac{\displaystyle\int_0^\infty C_p(t,z)(t-\mu_1)^2\,dt}{\displaystyle\int_0^\infty C_p(t,z)\,dt} \qquad (6)$$

## 2.3 Local particle velocity

As mentioned above, the measured particle velocity was hardly affected by the arrangements of the taps for introduction of tracer particles and the detection probes. Therefore, only the results obtained for the case where the tracer was introduced at 1800 mm and detected at 1900 and 2000 mm are shown in the following sections. The measurements were repeated from 16 to 30 times for each experimental condition. Most of the results for the particle velocity, $U_p$, under the same condition, fell within an error of $\pm5\%$; therefore, only the average value of the velocity is presented.

The dependence of the average local particle velocity on the superficial gas velocity under the fast fluidization condition ($U_g=150$–$215$ cm/s) is shown in **Fig. 8** together with the volume fraction of solids calculated from Eq. (1) using the pressure difference measured between 1900 and 2000 mm above the distributor. The particle velocity increased with increasing gas velocity.

In the series of runs, the total loading of particles in the system was kept constant. Thus the volume fraction of solids was reduced with increasing gas velocity as shown in Fig. 8, because the pressure drop through the cyclones increased.

The local particle velocity was also measured under a different total loading of particles in the system while the gas velocity was kept constant. The values of local particle velocity for gas velocities of 180, 200, and 215 cm/s are plotted against the measured volume fraction of solids in **Fig. 9.** For any gas velocity the local particle velocity was affected by the superficial gas velocity rather than the volume fraction of solids.

### 2.4 Axial dispersion coefficient

The values of the axial dispersion coefficient calculated from the two signals using Eqs. (3) and (4) fell within a wide range from 1 to 900 cm² for all experimental conditions employed in the present study. In the experimental results, no appreciable difference caused by difference in experimental conditions was observed. All data on the axial dispersion coefficient are shown in **Fig. 10.** The results suggest the unsteady and random behaviour of solids in the fast fluidized bed.

### 3. Discussion

The slip velocity between particle and gas is usually defined as

$$U_s = U_g/\varepsilon - U_p \qquad (7)$$

using the average particle velocity, average volume fraction and superficial gas velocity, while the local slip velocity is defined using local values. In the present study, the local particle velocity at the axis of the bed was directly measured, while the gas velocity used for the analyses was the superficial one. Though the local gas velocity, $U_g^*$, or the local volume fraction of solid, $1-\varepsilon^*$, at the center of the cross section was not measured, their values are evaluated as follows.

$$U_g^* > U_g \qquad (8)$$

$$1 - \varepsilon^* > 0 \qquad (9)$$

Thus the local slip velocity at the center of the cross section, $U_s^*$, is estimated as follows.

$$
\begin{aligned}
U_s^* &= U_g^*/\varepsilon^* - U_p \\
&> U_g^* - U_p \\
&> U_g - U_p
\end{aligned} \qquad (10)
$$

The measured values of $U_g - U_p$ were mostly larger than the value of the terminal velocity of a single particle, 10.2 cm/s. Therefore, the slip velocity at the axis of the bed is suggested to be larger than the value of the terminal velocity of a single particle.

### Conclusion

The behaviour of FCC particles was investigated in a fast fluidized bed of 50 mm internal diameter. When the gas velocity exceeded 150 cm/s, the clear surface of the bed disappeared and intensive backmixing of
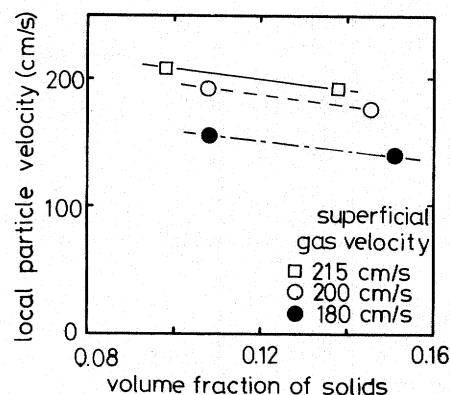


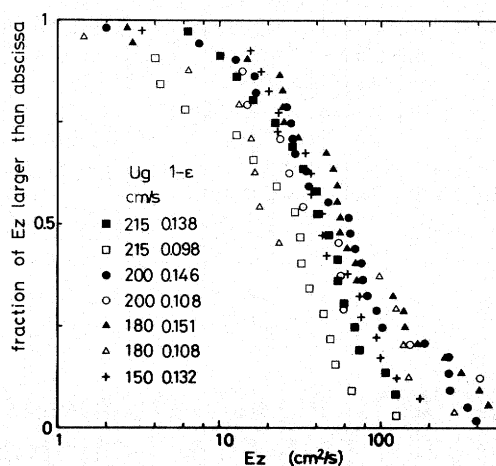**Fig. 9.** Effect of volume fraction of solids on local particle velocity



**Fig. 10.** Accumulated fraction of measured axial dispersion coefficient, $E_z$

solids was observed.

In the fast fluidization regime, local particle velocity as measured by an optical fiber system increased with increasing gas velocity, while the fraction of solids was reduced. The measured axial dispersion coefficient ranged from 1 to 900 cm²/s. Local slip velocity at the axis of the bed was mostly larger than the terminal velocity of a single particle.

**Nomenclature**

| | | |
|---|---|---|
| $C_p$ | = concentration of particles | [g cm⁻³] |
| $E_z$ | = axial dispersion coefficient of solids | [cm² s⁻¹] |
| $g$ | = acceleration of gravity | [cm s⁻²] |
| $h$ | = height | [cm] |
| $p$ | = static pressure | [g cm⁻¹ s⁻²] |
| $t$ | = time | [s] |
| $U_g$ | = superficial gas velocity | [cm s⁻¹] |
| $U_{mf}$ | = minimum fluidization velocity | [cm s⁻¹] |
| $U_p$ | = local particle velocity | [cm s⁻¹] |

| | | |
|---|---|---|
| $U_s$ | = slip velocity | $[\text{cm s}^{-1}]$ |
| $z$ | = distance | $[\text{cm}]$ |
| $\varepsilon$ | = void fraction | $[—]$ |
| $\mu_1$ | = first absolute moment | $[\text{s}]$ |
| $\mu_2$ | = second central moment | $[\text{s}^2]$ |
| $\rho_0$ | = particle density | $[\text{g cm}^{-3}]$ |

$\langle$Superscript$\rangle$

\* = local value at center of cross section

## Literature Cited

1) Furusawa, T., M. Suzuki and J. M. Smith: *Catal. Rev. Sci. Eng.*, **18**, 297 (1978).
2) Hartge, E.-U., D. Rensner and J. Werther: "Circulating Fluidizing Bed Technology II," ed. by J. F. Large and P. Basu, poster session, pp. 35–42 (1988).
3) Horio, M.: *Funtai Kogaku Kaishi*, **23**, 80 (1986).
4) Horio, M., K. Morishita, O. Tachibana and N. Murata: "Circulating Fluidizing Bed Technology II," ed. by J. F. Large and P. Basu, pp. 13–15 (1988).
5) Horio, M., A. Nonaka, M. Hoshiba, K. Morishita, Y. Kobukai, J. Naito, O. Tachibana, K. Watanabe and N. Yoshida: Proc. 1st Intern. Conf. on Circulating Fluidized Beds, p. 255, Nova Scotia (1985).
6) Ishida, M. and H. Hatano: "Saikin-no Kagaku Kougaku, Ryudoso Kogaku," p. 73, Gakkai Shuppan Center, Tokyo (1981).
7) Kuramoto, M., D. Kunii and T. Furusawa: *Powder Technol.*, **47**, 141 (1986).
8) Levenspiel, O.: "Chemical Reaction Engineering" 2nd ed. pp. 276–278, John wiley & Sons, New York (1972).
9) Lewis, W. K., E. R. Gilliland and W. C. Bauer: *Ind. Eng. Chem.*, **41**, 1104 (1949).
10) Morooka, S., K. Kawazuishi and Y. Kato: *Powder Technol.*, **26**, 75 (1980).
11) Reh, L.: *Chem. Eng. Progress*, **67** (2), 58 (1971).
12) Rhodes, M. J., P. Laussman, F. Villain and D. Geldart: "Circulating Fluidizing Bed Technology II." ed. by J. F. Large and P. Basu, pp. 20–25 (1988).
13) Takeuchi, H., T. Hirama, T. Chiba and L. S. Leung: Proc. World Cong. III of Chem. Eng., **3**, p, 477 (1986).
14) Yerushalmi, J., N. T. Cankurt, C. Geldart and B. Liss: *AIChE Symp. Ser.*, **74** (176) 1 (1978).
15) Yerushalmi, J. and A. M. Squires: *AIChE Symp. Ser.*, **73** (161) 44 (1977).
16) Yerushalmi, J., D. H. Turner and A. M. Squires: *Ind. Eng. Chem., Process Des. Dev.*, **15**, 47 (1976).
17) Youchou, Li and M. Kwauk: Proc. 1980 Intern. Fluidization Conf., p. 537, Plenum Press (1980).